Hysteresis of finite arrays of magnetic nanodots

M. Amin Kayali and Wayne M. Saslow
Department of Physics, Texas A & M University, College Station, Texas 77843-4242, USA
(Received 20 October 2003; revised manuscript received 21 June 2004; published 4 November 2004)

Hysteresis curves are investigated for finite arrays of $N\times N$ ferromagnetic nanodots subject to the dipole-dipole interaction ($N=2,\ldots,13$). Spin arrangements up to $N=6$ are presented, which indicate the onset of bulklike behavior associated with odd ($N=5$) and even ($N=6$) systems. The effect of field misalignment on the hysteresis loops is also studied for $N=3,\ldots,6$. The area A_N of the hysteresis loop is studied as a function of N. A_N-A_∞ approximately scales as $N^{-3/2}$ for N odd and as N^{-2} for N even.

DOI: 10.1103/PhysRevB.70.174404 PACS number(s): 75.40.Mg, 75.60.Ej, 75.60.Jk, 75.70.Kw

I. INTRODUCTION

A ferromagnetic particle goes into a monodomain state if its size D is below a critical value $D_c=10-100$ nm. This is due to the competition between the exchange and dipolar energies. Therefore, a nanoparticle in a monodomain state may be viewed as a giant magnetic dipole with magnetic moment of thousands of Bohr magnetons. For an $N\times N$ array of well-separated nanoparticles the exchange energy is usually negligible in comparison with the dipolar and anisotropy and Zeeman energies. The study of such systems is of increasing importance because of their technological applications in data storage devices and magnetic field sensors. As the technology of these devices moves towards higher densities of stored information, it requires smaller particles of magnetic media,[1,2] for which finite size effects become relevant. In finite arrays of such large dipole moment particles, the dipolar field of the array becomes comparable with the bulk anisotropy field. Dipolar effects in such systems affect the static and dynamics properties of the array; and thus must be taken into account.

The interest in magnetization processes and hysteretic behavior of finite arrays of nanoparticles in which the interaction between particles is mediated by the dipole-dipole interaction has grown in recent years. Ross *et al.*[3] experimentally studied the remanent states in cylindrical arrays of ferromagnetic nanoparticles as a function of the particle's size and the aspect ratio of the cylinder. They also performed micromagnetic simulations and showed that the remanent state is either a flower state or a magnetic vortex state depending on the size of the particles used and the aspect ratio of the cylinder.

Camley and Stamps in Refs. 4–6 investigated the dynamics and magnetization processes of a finite planar array of $N\times N$ ferromagnetic nanodots, for $N=3,4,5,6$. The nanodots were taken to interact only via the dipole-dipole interaction, and they were subject to an external field applied either along one side of the array or along its diagonal. They found rather complicated hystesresis loops with the magnetization reversal controlled by the shape anisotropy induced by the array itself.

We consider the same model, and extend their results, for $N=2,\ldots,13$. Our results for $N=3$ qualitatively agree with those of Ref. 4. We find that the behavior of these systems is surprisingly complex, both for smaller and for larger values of N, and we present the first systematic study of their $N\to\infty$ behavior. We obtain a scaling function for the hysteresis loop area as a function of N, for both odd and even N (which differ because only odd N has an uncompensated spin). We also study the dependence of the hysteresis loop on the inclination of the applied magnetic field with respect to one of the array sides.

In the present work each dot is taken to have a radius R_d, thickness d and a single degree of freedom corresponding to the orientation of a magnet of saturation magnetization M_0. We consider only the case of zero temperature. The dots are arranged on a square lattice with lattice spacing $a>2R_d$, and the dots interact only via the dipole-dipole interaction. The equation of motion for the magnetic moment of each dot is governed by the Landau-Lifshitz-Gilbert equation (LLG),[7] which reads

$$\frac{d\mathbf{M}}{dt}=\gamma\mathbf{M}\times\mathbf{H}_{\rm eff}-\alpha\frac{\mathbf{M}\times(\mathbf{M}\times\mathbf{H}_{\rm eff})}{M_s}, \tag{1}$$

where γ is the gyromagnetic ratio, α is the damping coefficient, $\mathbf{M}$ is the magnetic moment of the dot and $M_s=|\mathbf{M}|$ is the saturation magnetization, $\mathbf{H}_{\rm eff}$ is the average effective magnetic field acting on the dot. The average effective magnetic field acting on the ith dot is due to the applied external field, the dipolar fields, and the anisotropy field

$$\mathbf{H}^i_{\rm eff}=H_0\cos\theta\hat{x}+H_0\sin\theta\hat{y}-\mathbf{H}^i_{\rm dip}+2K_1\frac{m^i_z}{M^2}\hat{z}. \tag{2}$$

Here the dipole field acting on the ith dot due to all other dots in the array is given by

$$\mathbf{H}^i_{\rm dip}=h_{\rm dip}\sum_{j\neq i}\left(\frac{\mathbf{M}_j}{r^3_{ij}}-3\frac{(\mathbf{M}_j\cdot\mathbf{r}_{ij})\mathbf{r}_{ij}}{r^5_{ij}}\right), \tag{3}$$

where $h_{\rm dip}=\pi R_d^2 d/a^3$ is the strength of the dipole field and $\mathbf{r}_{ij}$ is in units of the lattice spacing a. For all arrays studied, we take $h_{\rm dip}=0.5$. The choice of anisotropy is determined by the shape of the dot, which in our problem is directed along the

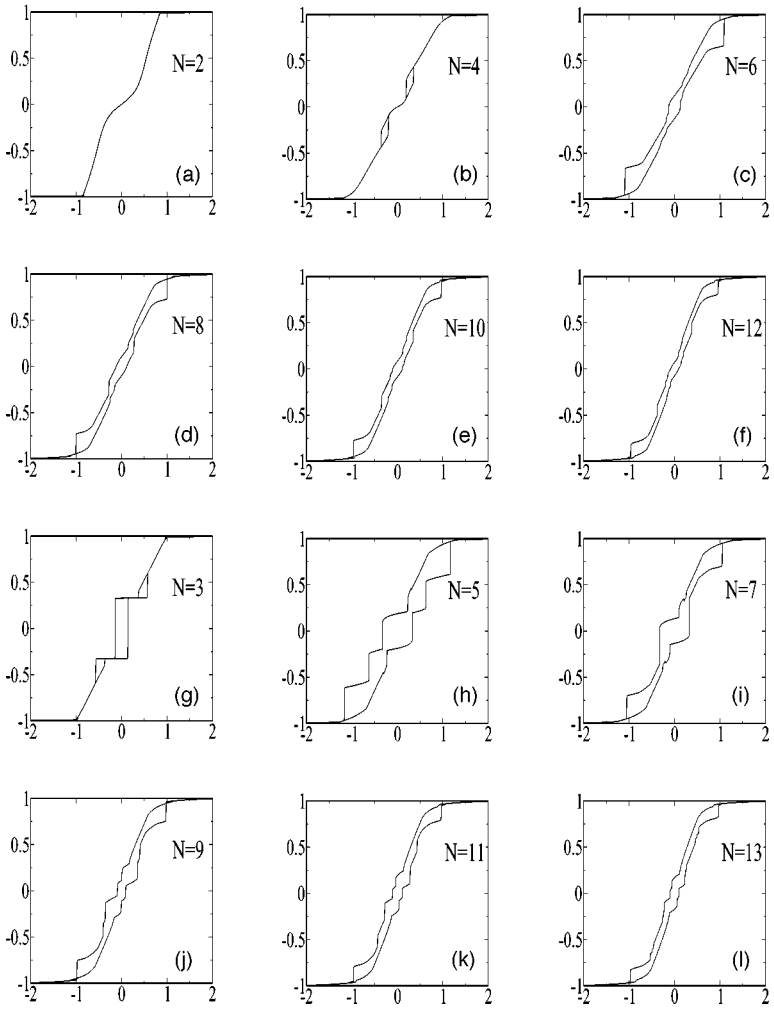

FIG. 1. Hysteresis loops $M(H)$, both in units of M_s, for weakly coupled arrays of $N\times N$ ferromagnetic nanodots. The external field is applied along the y axis, which coincides with one side of the array. The top two rows are for N even and the lower two are for N odd.

symmetry axis of the (cylindrical) dots. We divide both sides of Eq. (1) by (γM_s^2) and define a dimensionless time variable $\tau=\gamma M_s t$. The LLG in these reduced units becomes

$$\frac{d\mathbf{m}}{d\tau}=\mathbf{m}\times\mathbf{h}_{\text{eff}}-\frac{\alpha}{\gamma}\mathbf{m}\times(\mathbf{m}\times\mathbf{h}_{\text{eff}}), \tag{4}$$

where $\mathbf{m}=M/M_s$ and $\mathbf{h}_{\text{eff}}=\mathbf{H}_{\text{eff}}/M_s$. In our calculations, magnetic fields are measured in units of M_s and the energy is measured in units of $M_s^2a^3$.

This paper is organized as follows. Section II presents the numerical techniques we employed. Section III presents an extensive discussion of magnetization processes and hysteresis for arrays of $N\times N$ nanodots ($N=2,3,\ldots,13$) when the external field is applied along one side of the array. Section IV considers the effects of N even and N odd on the hysteresis loop of the finite array of nanodots. Section V considers the relationship between the area of the hysteresis loop and N. A brief summary is given in Sec. VI.

II. NUMERICS

We employ two different approaches to study the magnetization processes of our $N\times N$ arrays of nanodots. The first is the second order Runge–Kutta (RK) algorithm with fixed time step to integrate the LLG equation. The second is the "greedy algorithm." The two approaches yielded similar results.

In the RK approach, the integration employs a fixed time step $\Delta\tau=5\times10^{-3}$ and a damping coefficient $\alpha/\gamma=0.6$, with an initial state in which the magnetic moment of the dot is randomly generated. (The ground state of the system is unaffected by the value of α/γ; however, the choice of this ratio strongly affects the convergence and the computational time. For systems with many local minima, too large a value of α/γ could cause the algorithm to overshoot a local minimum, and too small a value of α/γ could cause the algorithm to get stuck in a local minimum. We found no indication of either effect in the present work.) Iterations are stopped when the difference between the total energy of the system from the $(n+1)$th iteration and that of the nth iteration is of the order of $\Delta E_n=10^{-5}$. Our solutions converged after almost 10^3 iterations.

The greedy algorithm takes the dot magnetization to align along the direction of the total local field. In the initial state each dot magnetization is chosen to point randomly. Next, the total local field is calculated for each dot. Finally, the magnetization for each dot is reoriented to point along its total local field. The convergence of the final state is checked in a manner similar to that used in the RK approach. We find

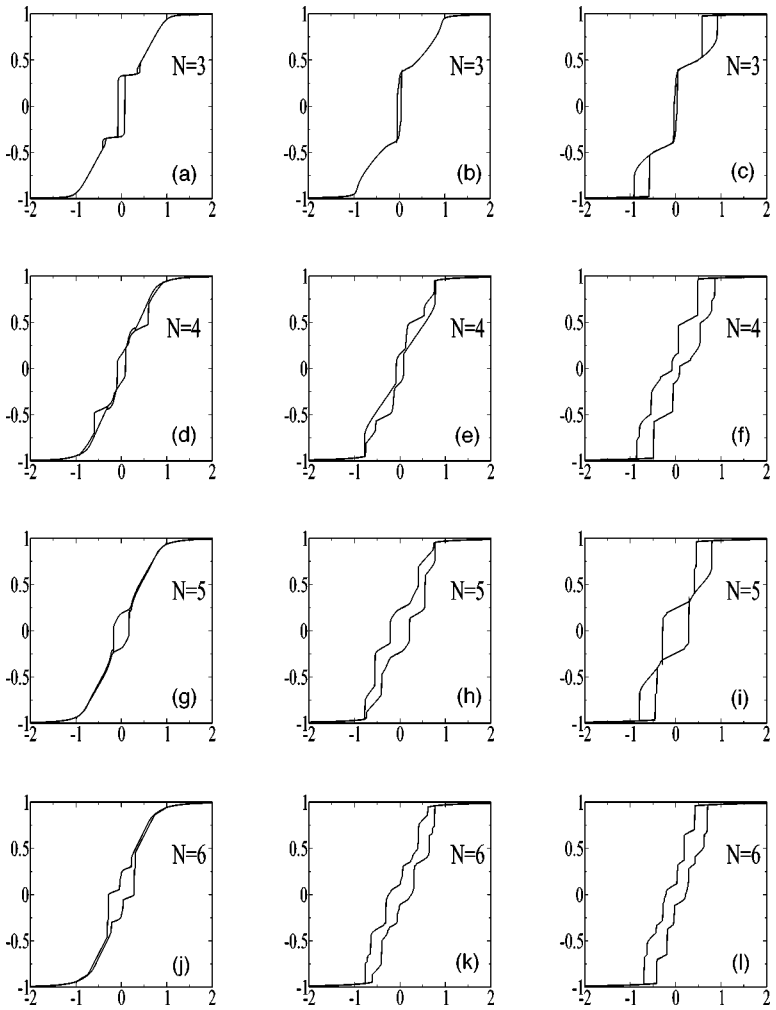

FIG. 2. Hysteresis loops $M(H)$, both in units of M_s, for $N=3\ldots,6$ arrays for the field at $\theta=5°, 30°$ and 45° going from left to right. For $\theta=0$ see Fig. 1.

that the LLG approach converges faster than the greedy algorithm. This is probably related to a phenomenon known in RLC circuits, where a critically damped circuit approaches equilibrium faster than a circuit with a larger amount of damping.

Calculation of the dipolar field at the *i*th dot is the most computationally time-consuming aspect of both approaches since it requires summation of the dipole fields from all other dots in the array. However, due to the relatively small sizes of our dot arrays this calculation is performed rather quickly.

III. HYSTERESIS LOOP AND EXTERNAL FIELD ORIENTATION EFFECT

Hysteresis loops $M(H)$ for $N\times N$ arrays of nanodots subject to an external magnetic field applied along one side have been calculated. Initially, a strong external field H_0 is applied to the array until saturation. The field is then decreased to $-H_0$, followed by an increase back to H_0. We take $H_0=2M_s$, and a fixed field-step of $\Delta H=2\times10^{-3}M_s$ is used in simulating the sweeping process. For each value of the external field the system was iterated until a stable final state is reached. As shown in Fig. 1, where $M(H)$ is plotted (both in units of M_s), the odd and even N arrays have somewhat different behaviors, especially for small N. One aspect of this is that, because of their unpaired spin, the odd-N systems display magnetization jumps as the field changes. The odd-N and even-N behavior becomes similar for larger values of N, something we study in a later section.

In Fig. 1, the angle of the field to one of the sides (the y axis) is taken to be $\theta=0$. Experimentally, however, field misalignment is almost inevitable, so that we also study field misalignment ($\theta\neq0$).

Figure 2 shows results for $N=3,\ldots,6$ and angles $\theta=5°$, 30°, and 45°. (We present only some ofthe more representative results; angles between 0° and 45° were studied in 5° increments.)

Comparison of Fig. 1 with Fig. 2 for $\theta=5°$ shows that a small misalignment of the applied field can change the hysteresis loop drastically.

For $N=3$, Fig. 2 shows that the central part of the hysteresis loop shrinks as θ increases. For $\theta=45°$, the central part almost disappears completely, and new small loops start to develop away from the center of the hysteresis loop. Our results for $N=3$ agree with those given in Ref. 4, which studied the cases $\theta=0°$ and 45°.

For $N=4$, at $\theta=0°$ there is no central loop, but there is a prominent loop at finite field. On the other hand, at $\theta=5°$, there is a central loop, and the finite field structure becomes rather complex. Further increase of θ leads to a filling out

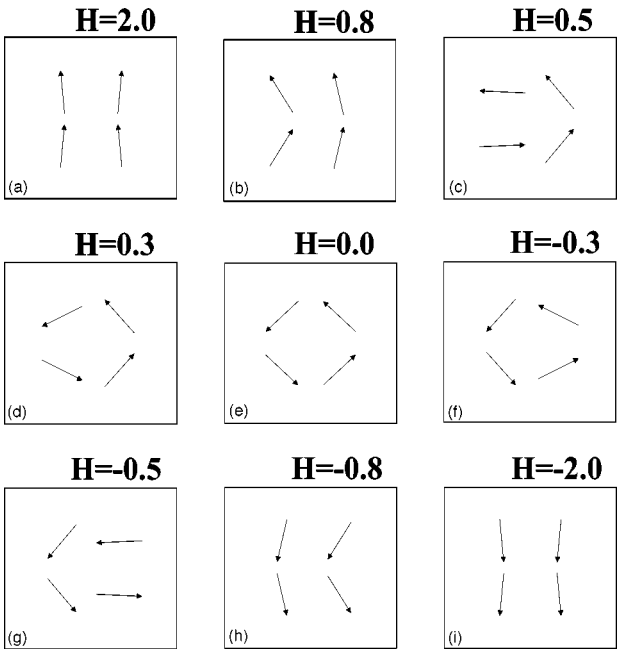

FIG. 3. Spin arrangements for an array of 2×2 ferromagnetic nanodots in external magnetic field.

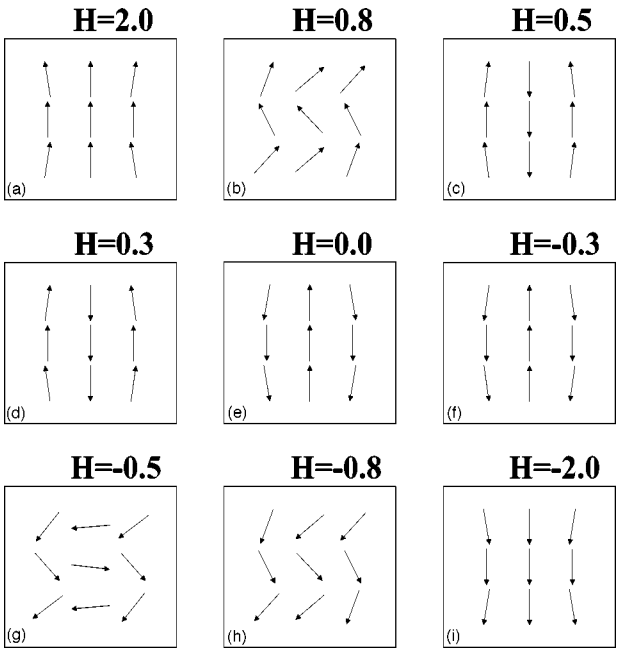

FIG. 4. Spin arrangements for an array of 3×3 ferromagnetic nanodots in an external magnetic field.

and connecting of various subloops. Also, note the appearance of jumps for nonzero θ.

For $N=5$, a small field misalignment has an enormous effect, at $\theta=5°$ shrinking the loop to a relatively small centralregion. As θ increases, the central loop grows, but the loop for $\theta=45°$ pinches off to yield three subloops, as for $N=3$.

For $N=6$, again a small field misalignment has an enormous effect, at $\theta=5°$ shrinking the loop to a relatively small centralregion. As θ increases, the central loop grows, but in contrast to $N=5$, the loop for $\theta=45°$ does not pinch off, and closely resembles the loop for $N=4$.

These different types of behavior indicate that this is a complex system, for which it is difficult to generalize.

IV. HYSTERESIS AND EVEN-ODD SIGNATURE IN FINITE ARRAY OF NANODOTS

In the absence of an external magnetic field the array of $N\times N$ nanodots favors antiferromagnetic ordering, thus minimizing its magnetostatic energy. A large external magnetic field applied to the array tends to orient the magnetic moments along the field, thus minimizing the Zeeman field energy. However, the spins at the array corners tip by a small angle, as shown in Figs. 3–6, forming a two-dimensional "flower" state.[8,9] The flower state persists until the applied field falls to $H_0=M_s$. For lower values of the applied field, the competition between the dipole-dipole interaction and the Zeeman energy becomes significant, and changes the array ordering.

For $N=2$, Fig. 3 shows that for $0<H_0<M_s$ the spins form a snakelike domain structure that winds either clockwise or counterclockwise. For $H_0=0$, the array has zero net per-dot magnetization, due to a vortexlike structure that persists for $-3M_s\leqslant H_0\leqslant 0.3M_s$.

The $N=3$ array was analyzed by Camley and Stamps in Ref. 4. This array also shows snakelike arrangements below $H_0=M_s$. For $H_0=0$ the final state of the array shows what we call a "barrel" state in which the spins at the left and right columns are oriented opposite to the central column with a slight tipping of the corner spins, as shown in Fig. 4. This agrees with Ref. 4 except that Ref. 4 shows no tipping of the corner spins. We have confirmed our numerics by making a small tipping angle expansion of the energy with the spins nearly but not completely aligned, and finding the tipping

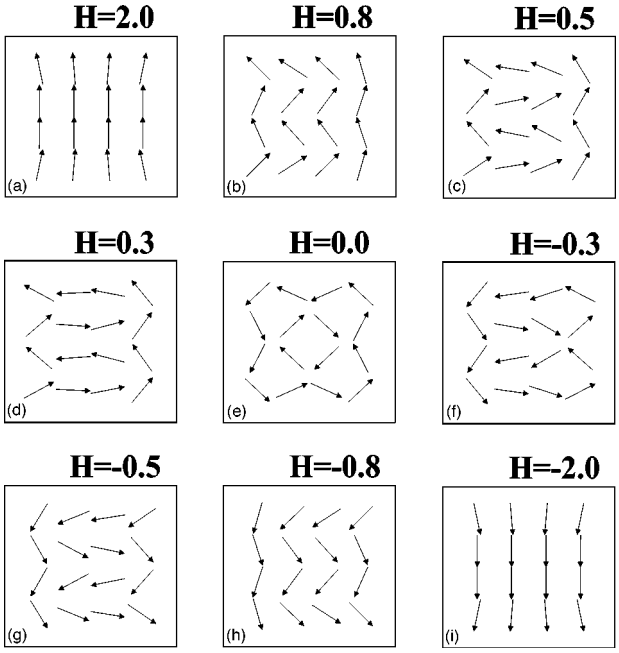

FIG. 5. Spin arrangements for an array of 4×4 ferromagnetic nanodots in external magnetic field.

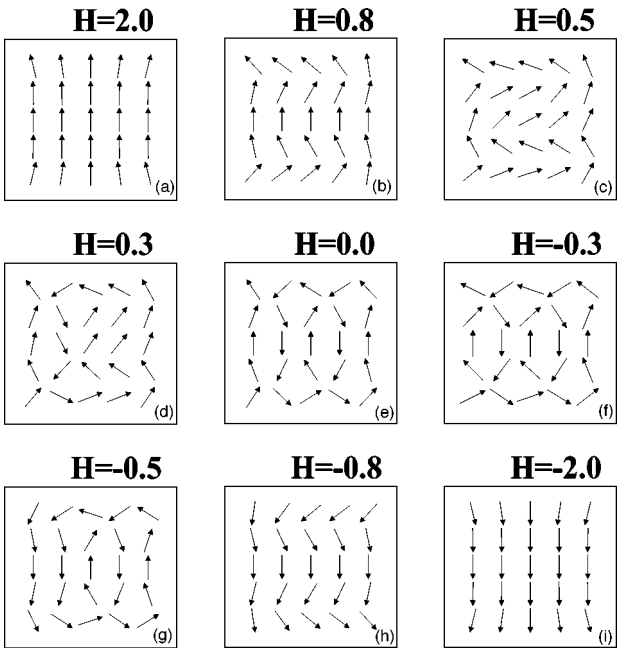

FIG. 6. Spin arrangements for an array of 5×5 ferromagnetic nanodots in external magnetic field.

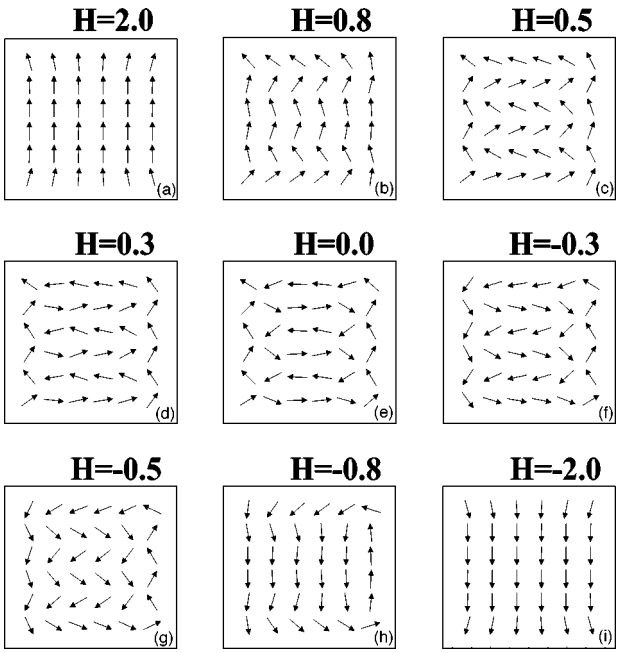

FIG. 7. Spin arrangements for an array of 6×6 ferromagnetic nanodots in external magnetic field.

angle that minimizes the energy. In both the numerics and in the minimization the corner spin tipping angle is (to five places) $|\alpha|=9.1115°$. The spin snapshots in Fig. 4 and the hysteresis loop analysis both show that the barrel state switches to an inverted barrel state when the applied field changes sign, as expected for the unpaired spin of the $N=3$ system.

Figure 5 shows that the $N=4$ array also features snakelike arrangements of the spins, for intermediate values of the applied field. However, in zero field the total per-dot magnetization is zero, which can be attributed to the formation of a vortex in the array's central 2×2block. The magnetic moments of the rest of the dots in the array form a ring that surrounds the vortex with opposite circulation. This state is stable for applied fields H_0 satisfying $-0.2M_s\leqslant H_0\leqslant0.2M_s$.

For all N, the flower state appears at high fields (here, $|H_0|=2.0M_s$). The hysteresis loops shown in Fig. 1 show a subtle difference in shape between arrays with odd N and arrays with even N. For odd N the loops show well-defined jumps whereas for even N this behavior is absent. This behavior is due to unpaired spins with uncompensated dipole fields. The jumps become less apparent for large N, where the distinction between even and odd N becomes unimportant.

When an array was placed in zero external field and given random initial conditions, the solutions converged to the same states as obtained in the hysteresis-cycle calculations, up to the degeneracy of the system. Thus, for $N=2,4$ there are two degenerate metastable states of opposite chirality (winding) with zero net magnetization in zero field, each of which has a fourfold rotational symmetry. For $N=6$ there are two degenerate states of opposite chirality, with nonvanishing net magnetization, each of these states has no apparent rotational symmetry. For $N=3$ there are two degenerate barrel states, with no rotational symmetry, and $N=5$ is similar to $N=6$. The hysteresis loop area A_N will produce further evidence that large system behavior commences with $N=5$ and $N=6$. Metastable states with vanishing net magnetization may appear for arrays with even N. However, our simulations showed that these states appear only for $N=2,4$. For arrays with odd N the unpaired dipoles prevent the occurence of such states.

V. HYSTERESIS LOOP AREA A_N VS PARTICLE NUMBER N

Although the area of the hysteresis loop A_N tends to zero for the $N=2$ array, it is clearly nonzero for all other arrays. Figure 8 presents the hysteresis loop areas as circles (N even) and squares (N odd). Figure 8 shows that the area of the hysteresis loop decreases with increasing N except for $N=3$ for N odd and $N=2,4$ for N even. The $N=5$ and $N=6$ arrays, which are the first to show something like bulk behavior,

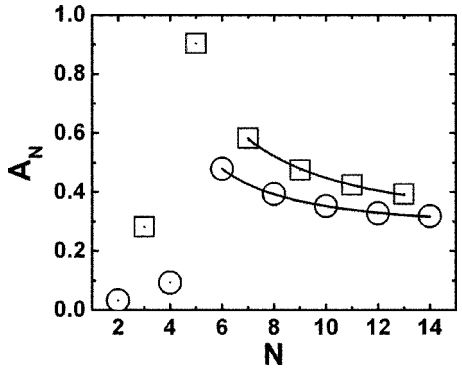

FIG. 8. The area of the hysteresis loop as a function of the number of particles N.

TABLE I. Fitting parameters for data given in Fig. 8, using Eq. (5).

N	A_∞	C	p
Even	0.278	6.31 ± 0.42	1.95 ± 0.03
Odd	0.278	6.92 ± 0.86	1.61 ± 0.06

have maximum A_N for odd and even, respectively; their spin arrangements are given in Figs. 6 and 7. We have fitted our data to the asymptotic form

$$A_N = A_\infty + \frac{C}{N^p}, \tag{5}$$

where A_∞, C, and p are constants to be determined. If larger values of N had been computationally feasible, we would have considered only large values of N for the fit. In practice, for N odd the data are fit starting from $N=7$ and for N even from $N=6$. (The fit is not as good when $N=5$ is included, so we do not show this case.) Both fits are shown as solid lines in Fig. 8, where the values of A_∞, C, and p are given in Table I. The fits have values of χ^2 that are less than 10^{-5}.

For odd N, A_N varies approximately as $A_N \sim N^{-3/2}$ whereas for even N it varies approximately as N^{-2}. We attribute no fundamental significance to these exponents, although the difference surely can be traced to the effect of the unpaired spin for odd N.

VI. SUMMARY

We have studied the hysteresis and magnetization processes for $N \times N$ arrays (with $N=2,\ldots,13$) of uniaxial ferromagnetic nanodots interacting via the dipole-dipole interaction. For an external magnetic field aligned or misaligned with one side of the array, the hysteresis loops are surprisingly complex. For arrays with odd N the hysteresis loops possess jumps, whereas for even N they do not. As N increases, the area A_N of the hysteresis loop begins to saturate, approaching a nonzero finite value determined from a data fit. The area of the hysteresis loop scales with N approximately as $N^{-3/2}$ for N odd, and approximately as N^{-2} for even.

ACKNOWLEDGMENTS

The authors would like to thank V. L. Pokrovsky, A. S. Kirakosyan, and S. Erdin for fruitful discussions. This work was supported by NSF Grants Nos. DMR 0103455 and DMR 0072115, DOE Grant No. DE-FG03-96ER45598, and by the Telecommunication and Information Task Force at Texas A&M University.

[1] E. C. Stoner and E. P. Wohlfarth, Philos. Trans. R. Soc. London, Ser. A **240**, 599 (1948).
[2] J. F. Smyth, S. Schultz, D. R. Fradkin, D. P. Kern, S. A. Rishton, H. Schmid, M. Cali, and T. R. Koehler, J. Appl. Phys. **69**, 5262 (1991).
[3] C. A. Ross, M. Hwang, M. Shima, J. Y. Cheng, M. Farhoud, T. A. Savas, H. I. Smith, W. Schwarzacher, F. M. Ross, M. Redjdal, and F. B. Humphrey, Phys. Rev. B **65**, 144417 (2002).
[4] R. L. Stamps and R. E. Camley, Phys. Rev. B **60**, 11694 (1999).
[5] R. L. Stamps and R. E. Camley, Phys. Rev. B **60**, 12264 (1999).
[6] R. L. Stamps and R. E. Camley, J. Magn. Magn. Mater. **177–181**, 813 (1998).
[7] E. M. Lifshitz and L. P. Pitaevskii, *Course of Theoretical Physics Vol. 5: Statistical Physics* (Pergamon, New York, 1980), Part 2.
[8] A. Aharoni, *Introduction to the Theory of Ferromagnetism* (Oxford University Press, Oxford, 2001).
[9] V. Ternovsky,B. Luk'yanchuk, and J. P. Wang, Pis'ma Zh. Tekh. Fiz. **73**, 746 (2001) [JETP Lett. **73**, 661 (2001)].